Phys Chem Minerals (2002) 29: 166–169
DOI 10.1007/s00269-001-0224-4

ORIGINAL PAPER

J. Li · H. K. Mao · Y. Fei · E. Gregoryanz
M. Eremets · C. S. Zha

Compression of Fe_3C to 30 GPa at room temperature

Received: 30 April 2001 / Accepted: 17 September 2001

Abstract Polycrystalline Fe_3C (cementite) was compressed in a neon pressure medium to 30.5 GPa at 300 K using diamond-anvil cell techniques. Angular dispersive X-ray diffraction of Fe_3C was measured using monochromatic synchrotron radiation and imaging plates. No phase transition was observed up to the highest pressure studied. The pressure–volume data were fitted to a third-order Birch–Murnaghan equation of state. With V_0 constrained to a measured value of 155.28 $Å^3$, the best fit yielded a 300-K isothermal bulk modulus $K_0 = 174 \pm 6$ GPa, and its pressure derivative at constant temperature $K_0' = (\partial K_0/\partial P)_T = 4.8 \pm 0.8$.

Keywords Fe_3C · High pressure · Phase stability · Bulk modulus · EoS

Introduction

Fe_3C is orthorhombic (space group *Pnma*) at 1 bar and 300 K (PDF no. 35-0772). Its diffraction pattern consists of many closely spaced reflections. Due to experimental difficulties with high-resolution X-ray diffraction measurements under hydrostatic conditions, compression data for Fe_3C are sparse. Jephcoat and Besedin (1996) reported that no pressure-induced phase transition in Fe_3C was observed up to 21 GPa, but they did not provide any pressure–volume data. Recently, two investigations on Fe_3C were carried out simultaneously. Scott et al. (2001) measured the P–V relation of Fe_3C using a methanol–ethanol–water mixture (16:3:1 by volume) as a pressure-transmitting medium, coupled with external heating to relax pressure gradients. They found no phase transitions up to 73 GPa, and determined the bulk modulus of Fe_3C and its pressure derivative. It is known that at room temperature, the methanol–ethanol–water mixture freezes at 14.4 GPa (Fujishiro et al. 1982). Upon solidification, the viscosity of the methanol–ethanol–water mixture increases rapidly and can support relatively large nonhydrostatic stress (Piermarini et al. 1973; Fujishiro et al. 1982; Downs et al. 1996; Scott et al. 2001). Theoretical (Singh et al. 1998) and experimental (e.g., Meng et al. 1993; Downs et al. 1996; Zha et al. 2000) studies have shown that the presence of nonhydrostatic stress leads to systematic errors in lattice parameter determination by X-ray diffraction using a diamond-anvil cell. Since Fe_3C is of low symmetry and has accordingly closely spaced diffraction peaks, any difference in non-hydrostaticity is expected to exaggerate differences in the measured P–V relation. To improve the accuracy and precision of the equation of state of Fe_3C, we studied the compression of Fe_3C from 1 bar to 30.5 GPa at 300 K, using neon as a pressure-transmitting medium. At 300 K, neon is fluid and is truly hydrostatic below 4.7 GPa (Finger et al. 1981). Above 4.7 GPa, crystalline neon is relatively weak and stays quasihydrostatic to at least 78 GPa (Bell and Mao 1981; Jephcoat 1986; Zha et al. 2000). Therefore, above the freezing pressure of the methanol–ethanol–water mixture, neon provides a higher degree of hydrostaticity.

J. Li (✉) · H. K. Mao · Y. Fei
E. Gregoryanz · M. Eremets
Geophysical Laboratory and Center for High-Pressure Research,
Carnegie Institution of Washington,
5251 Broad Branch Rd. NW,
Washington DC 20015, USA
e-mail: jieli@gl.ciw.edu
Tel.: +1-202-478-8933; Fax: +1-202-478-8901

C. S. Zha
Cornell High Energy Synchrotron Source (CHESS),
Cornell University, Ithaca, NY 14853, USA

Experimental method

The starting material was polycrystalline Fe_3C synthesized from pure iron and graphite powder in a MgO capsule at 2 GPa and 1273 K, using a piston-cylinder device at the Geophysical

Laboratory. X-ray diffraction measurements and electron microprobe analyses confirmed that the structure and composition of the run product matches that of cementite.

High pressure was generated in a Mao–Bell type diamond-anvil cell with 500 μm culet size (Mao et al. 1979). Prior to sample loading, a piece of T301 stainless steel gasket was compressed in the cell to 20 GPa and 30 μm in thickness. A 200-μm hole was drilled in the pre-indented gasket, forming a sample chamber. A pellet of Fe_3C powder (100 μm in diameter, 10 μm in thickness) and a few grains of ruby powder were loaded in the center of the sample chamber between two diamond anvils. The sample chamber was then filled with pressurized neon gas at 0.2 GPa using a high-pressure gas-loading apparatus (Jephcoat et al. 1987) and sealed at 2 GPa. Neon serves as a hydrostatic and quasihydrostatic pressure medium over the pressure range of this study.

Pressure was measured from the calibrated wavelength shifts in the R_1 line of the laser-induced fluorescence spectra of ruby ($\Delta\lambda$) using the following relation:

$$P = A/B\left\{[1 + (\Delta\lambda/\lambda_0)]^B - 1\right\}\ , \quad (1)$$

where A = 1904 GPa, B = 7.715, and λ_0 = 694.3 nm (Zha et al. 2000). Within the experimental pressure range, the precision of the ruby pressure scale is ±0.2 GPa (Hemley et al. 1989). Small variations in pressure during each diffraction measurement were incorporated in the uncertainty. Room temperature was 300 ± 1 K.

Angular dispersive X-ray diffraction measurements were carried out at a wiggler beam line at the C-1 station, Cornell High Energy Synchrotron Source (CHESS). An incident monochromatic beam (energy 25.02 ± 0.02 keV) was generated by a Si (111) monochromator, and calibrated by scanning the absorption edge of a Ag film. The beam was collimated to a diameter of 25 μm. The direct beam passes through both diamond anvils, the sample and a lead (Pb) filter, and marks its position on an imaging plate that is placed perpendicular to the beam path. Diffraction data were collected on the imaging plate, for an exposure time of 10 to 30 min. The imaging plate was read by a Fuji BAS 2000 scanner with a 100 × 100 μm pixel size, which digitizes an 8″ × 10″ area into approximately 2048 × 2560 pixels. Debye–Scherrer rings recorded on the imaging plate were integrated to produce a conventional powder spectrum using the FIT2D program (Hammersley et al. 1996). A gold standard was used to determine the distance between the sample and the imaging plate.

Results and discussion

No reflections of neon were observed below 7.9 GPa, as neon was fluid or had coarse crystallinity. At and above 7.9 GPa, at least one reflection of neon (2 2 0) was present in each diffraction spectrum, from which the lattice parameter of neon was calculated (Table 1). The pressure of neon based on its unit-cell volume (Hemley et al. 1989) agrees with that measured by the ruby scale within uncertainties. However, the neon pressure is systematically lower than the ruby pressure, and the difference increases with pressure. To minimize the error, we took the average of the neon and ruby pressure as the pressure of Fe_3C.

More than 18 peaks of Fe_3C were identified in each diffraction spectrum. As pressure increased, all the peaks shifted continuously toward higher 2θ (smaller d-spacing), but the overall pattern did not change. Since no indication of a phase transition was observed, we assumed the 1-bar cementite structure for lattice parameter determination. Both individual-peak and whole-profile fitting methods were used. With the individual-peak method, we located peak positions using a peak-fitting program, then refined lattice parameters using a least-squares method. Excluding peaks with very low intensity and/or strong overlap, five or more peaks out of the set [(0 0 2), (2 1 0), (2 1 1), (1 0 2), (2 2 0), (0 3 1), (1 1 2), (1 3 1), (2 2 1), (1 2 2), (2 3 0), (3 0 1)] were used for refinement. Depending on the choice of peaks, the refined lattice parameters vary by as much as ±0.002 Å on a, ±0.015 Å on b, and ±0.004 Å on c. The variations in a, b, and c tend to cancel out so that the calculated unit-cell volume is less sensitive to the choice of peaks. For whole-profile fitting, we used the

Table 1 Lattice parameters and unit-cell volume of Fe_3C and neon (300 K)

P (GPa)	±	Fe_3C				Ne
		a (Å)	b (Å)	c (Å)	V (Å)^3	a (Å)
0.000100[a]		5.091	6.7434	4.526	155.40	
0.000100	(1)[b]	5.087 (1)	6.752 (2)	4.521 (1)	155.28 (11)	
2.5	(2)	5.063 (1)	6.720 (2)	4.498 (1)	153.04 (11)	
4.9	(2)	5.044 (1)	6.697 (2)	4.481 (1)	151.37 (11)	
7.9	(3)	5.022 (1)	6.658 (2)	4.456 (1)	148.99 (11)	3.652 (1)
10.9	(4)	5.000 (1)	6.621 (2)	4.436 (1)	146.85 (11)	3.563 (1)
13.4	(6)	4.982 (1)	6.604 (2)	4.421 (1)	145.46 (11)	3.504 (1)
17.2	(8)	4.960 (1)	6.574 (2)	4.399 (1)	143.44 (11)	3.436 (1)
19.5	(9)	4.940 (2)	6.556 (4)	4.378 (2)	141.79 (21)	3.400 (1)
22.1	(9)	4.924 (1)	6.526 (4)	4.365 (1)	140.27 (15)	3.366 (1)
24.3	1.0	4.910 (1)	6.516 (2)	4.356 (1)	139.36 (10)	3.340 (1)
27.2	1.1	4.896 (1)	6.497 (4)	4.342 (1)	138.12 (15)	3.311 (1)
30.3	1.2	4.882 (2)	6.476 (4)	4.325 (1)	136.74 (17)	3.282 (1)
30.5	1.2	4.877 (1)	6.480 (2)	4.325 (1)	136.68 (10)	3.280 (1)

[a] PDF no. 35-0772

[b] The *numbers in parentheses* are uncertainties on the last digit(s). The uncertainties in pressure are estimated from the precision of the ruby scale (Hemley et al. 1989), the precision of pressure calibration based on the equation of state of neon (Hemley et al. 1989), and include small pressure variations during each diffraction measurement, as well as the difference between the neon and ruby pressure. The uncertainties in the lattice parameters of Fe_3C reflect the reproducibility using the individual peak and whole-profile fitting methods, and the reproducibility of duplicate measurements at nearly identical pressures. The uncertainties in lattice parameters of neon are due to errors in the calibration of experimental geometry and a secondary source of errors in peak fitting

Le Bail method implemented in GSAS (Larson and von Dreele 1998). Figure 1 shows comparisons between fitted and observed diffraction spectra at 4.9 and 30.5 GPa. The overall fit is reasonable even at the highest pressure. Small discrepancies are probably due to inadequate parameterization of peak profiles. The results of Le Bail fitting are reproducible to ± 0.001 Å for all three lattice parameters. In most cases, they also agree with results of the individual peak method using all 12 peaks.

The unit-cell volume and lattice parameter results of Le Bail fitting are listed in Table 1 and plotted against pressure in Figs. 2 and 3. In the upper right inset of Fig. 2, an *F–f* plot based on the Birch–Murnaghan equation of state (Heinz and Jeanloz 1984; Angel 2000) indicates that both a second- and a third-order equation of state would fit our data. We fitted the *P–V* data to a third-order Birch–Murnaghan equation of state:

$$P = \frac{3}{2}K_0\left[\left(\frac{V_0}{V}\right)^{\frac{7}{3}} - \left(\frac{V_0}{V}\right)^{\frac{5}{3}}\right]\left\{1 - \frac{3}{4}(4 - K_0')\left[\left(\frac{V_0}{V}\right)^{\frac{2}{3}} - 1\right]\right\}, \quad (2)$$

where V_0 and K_0 are the volume and isothermal bulk modulus at 1 bar and 300 K, respectively, and K_0' is the first pressure derivative of K_0 at 300 K. Using our measured V_0, a least-squares fit yielded $K_0 = 174 \pm 6$ GPa and $K_0' = 4.8 \pm 0.8$. The tradeoff between K_0 and K_0' is shown in the lower left inset of Fig. 2.

Linear compressibility [$\beta_0 = -(\partial l/\partial P)_{P=0}/l_0$, where l_0 is the length of a unit-cell axis at 1 bar] was estimated by fitting the axial compression data of Fe_3C to a linearized third-order Birch–Murnaghan equation of state (Angel 2000). Using our measured a_0, b_0, c_0 and the fitted K_0' to our *P–V* data, we found that the linear compressibilities along three axes are similar: $\beta_0^a = 0.00184(2)$ GPa^{-1}, $\beta_0^b = 0.00191(2)$ GPa^{-1}, $\beta_0^c = 0.00200(2)$ GPa^{-1} (Fig. 3).

Carbon is a possible component of the Earth's core. Wood (1993) proposed that the Earth's inner core may be a carbide compound. One of his arguments was that the

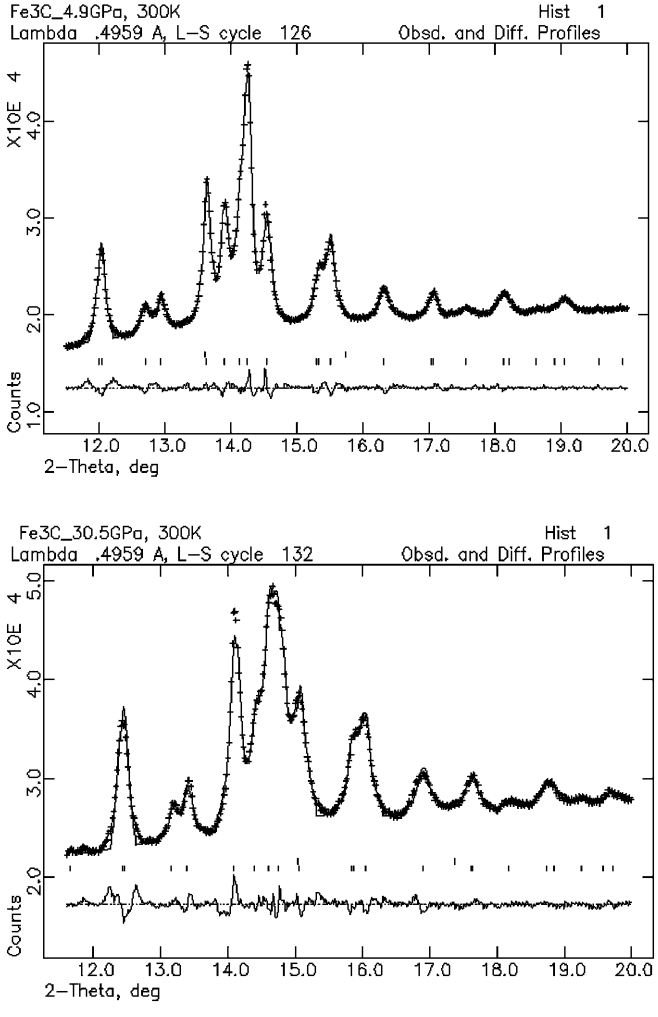

Fig. 1 Le Bail fits (*curves*) to integrated X-ray diffraction spectra (*crosses*) at 4.9 (*top*) and 30.5 GPa (*bottom*) and 300 K. *Tick marks* show the positions of calculated reflections of neon (*above*) and Fe_3C (*below*). The difference between the observed and fitted profiles is shown *below the tick marks*

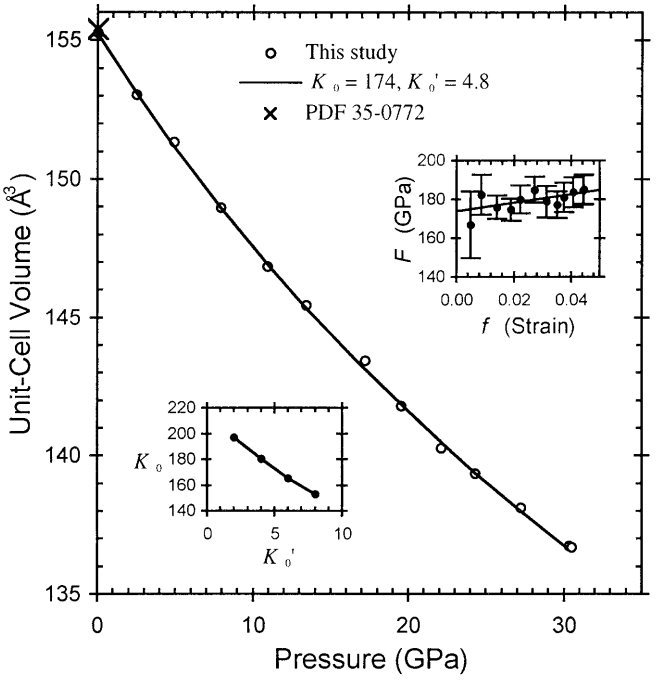

Fig. 2 Pressure–volume data of Fe_3C at 300 K. *Open circles* are experimental results from this study (Table 1). The *cross* is a reference point based on PDF no. 35-0772. The *curve* represents the best fit to our data using a third-order Birch–Murnaghan finite-strain expansion, as described in the text. The *upper right inset* is a plot of a normalized pressure *F* versus strain *f* (Heinz and Jeanloz 1984; Angel 2000). The *line* is a third-order finite strain fit to our data. The *error bars* are calculated from the uncertainties in pressure and volume (Table 1). The *lower left inset* shows the dependence of K_0 on K_0'. The *solid curve* is a trendline drawn through the data points (*solid circles*). The *error bars* are smaller than the symbols

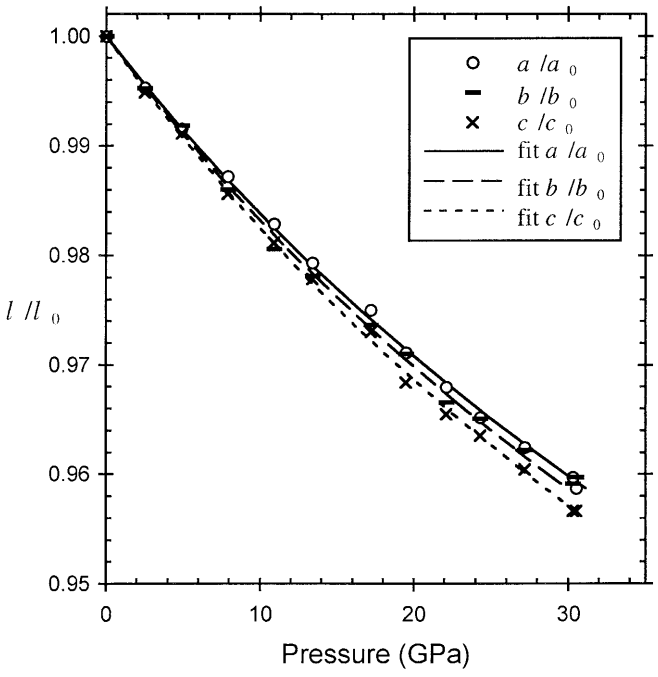

Fig. 3 Axial compression data of Fe_3C at 300 K. The *curves* are best fits to our data using linearized third-order Birch–Murnaghan equations of state, as described in the text

estimated density of Fe_3C is in good agreement with that of the inner core at the corresponding pressures and temperatures. As no data on the phase stability and bulk modulus of Fe_3C were then available, Wood assumed that the structure of Fe_3C at ambient condition persists to the inner core conditions, and estimated the high-pressure density of Fe_3C based on carbide systematics. Our results confirm that the structure of Fe_3C stays orthorhombic up to 30.5 GPa at 300 K. Our measured bulk modulus and its pressure derivative at 300 K agree with the estimates of Wood ($K_0 = 174$ GPa, $K_0' = 5.0$, 1993), as well as with the experimental results of Scott et al. ($K_0 = 175 \pm 4$ GPa, $K_0' = 5.2 \pm 0.3$, 2001). These data are important for evaluating the possibility of Fe_3C as a major component of the Earth's inner core. However, the experimental pressures reached to date are far from those of the Earth's inner core, and the effect of temperature is barely known.

Although our equation-of-state parameters are similar to those obtained by Scott et al. (2001), the data precision and thus the confidence level for extrapolation to core conditions have been greatly improved in the present study. Comparing the X-ray diffraction spectra from the two studies, it is evident that at pressures higher than 16 GPa, Fe_3C peaks using the methanol–ethanol–water mixture pressure medium coupled with external heating are considerably less resolved than those using neon. For example, at 30.5 GPa, the FWHM of Fe_3C peak (112) using the methanol–ethanol–water mixture plus heating is three times that of using neon. The higher resolution leads to a more accurate equation of state, and tighter constraints on inner core models.

Acknowledgements This work is supported by the NSF grant (EAR 0001173), the NASA grant (NAGW-3942), and by the Carnegie Institution of Washington. The authors wish to thank R. Von Dreele, M. Koch-Müller, and P. Dera for their help with the GSAS program; C. Prewitt and R. Angel for suggestions on EoS fitting; S. Desgreniers and C. Sanloup for their help with imaging-plate analysis; H. Scott for discussions; and the personnel at Cornell High Energy Synchrotron Source (CHESS) for the facility and technical assistance. We also thank R. Hemley and two anonymous reviewers for their critical and constructive comments on the manuscript.

References

Angel R (2000) Equations of state. In: Hazen RM, Downs RT (eds) High-temperature and high-pressure crystal chemistry. Reviews in Mineralogy, Mineralogical Society of America, vol 41, pp 35–60

Bell PM, Mao HK (1981) Degree of hydrostaticity in He, Ne, and Ar pressure-transmitting media. Carnegie Inst. Washington Yb 80, 404–406

Downs RT, Zha CS, Duffy TS, Finger LW (1996) The equation of state of forsterite to 17.2 GPa and effects of pressure media. Am Mineral 81: 51–55

Finger LW, Hazen RM, Zou G, Mao HK, Bell PM (1981) Structure and compression of crystalline argon and neon at high pressure and room temperature. Appl Phys Lett 39: 892–894

Fujishiro I, Piermarini GJ, Block S, Munro RG (1982) Viscosities and glass transition pressures in the methanol-ethanol-water system. In: Backman CM, Johannisson T, Tegnér L (eds) High pressure in research and industry. Arkitektkopia, Uppsala, pp 608–611

Hammersley AP, Svensson SO, Hanfland M, Fitch AN, Häusermann D (1996) Two-dimensional detector software: from real detector to idealized image or two-theta scan. High Press Res 14: 235–248

Heinz DL, Jeanloz R (1984) The equation of state of the gold calibration standard. J Appl Phys 55: 885–892

Hemley RJ, Zha CS, Jephcoat AP, Mao HK, Finger LW (1989) X-ray diffraction and equation of state of solid neon to 110 GPa. Phys Rev (B) 39: 11 820–11 827

Jephcoat AP (1986) Static compression of iron to 78 GPa with rare solids at pressure-transmitting media. J Geophys Res 91: 4677–4684

Jephcoat AP, Besedin SP (1996) Equation of state of Fe_3C, NiH_x and ReH to high pressures (abstract). Eos Trans AGU 77: 674

Jephcoat AP, Mao HK, Bell PM (1987) Operation of the megabar diamond-anvil cells. In: Ulmer GC, Barns HL (eds) Hydrothermal experimental techniques. Wiley, New York, pp 469–506

Larson AC, von Dreele RB (1998) GSAS: general structure analysis system. Los Alamos National Laboratory

Mao HK, Bell PM, Dunn KJ, Chrenko RM, De Vries C (1979) Absolute pressure measurements and analysis of diamonds subjected to maximum static pressures of 1.3–1.7 Mbar. Rev Sci Instrum 50: 1002–1009

Meng Y, Weidner DJ, Fei Y (1993) Deviatoric stress in a quasi-hydrostatic diamond anvil cell: effect on the volume-based pressure calibration. Geophys Res Lett 20(12): 1147–1150

Piermarini GJ, Block S, Barnett JD (1973) Hydrostatic limits in liquids and solids to 100 kbar. J Appl Phys 44(12): 5377–5382

Scott HP, Williams Q, Knittle E (2001) Stability and equation of state of Fe_3C to 73 GPa: implications for carbon in the Earth's core. Geophys Res Lett 28(9): 1875–1879

Singh AK, Balasingh C, Mao HK, Hemley RJ, Shu J (1998) Analysis of lattice strains measured under non-hydrostatic pressure. J Appl Phys 83(12): 7567–7575

Wood BJ (1993) Carbon in the core. Earth Planet Sci Lett 117: 593–607

Zha CS, Mao HK, Hemley RJ (2000) Elasticity of MgO and a primary pressure scale to 55 GPa. Proc Natl Acad Sci 97: 13 494–13 499